Annals of Glaciology

Article

Cite this article: Orheim O, Giles AB, Jacka TH (Jo), Moholdt G (2023). Quantifying dissolution rates of Antarctic icebergs in open water. *Annals of Glaciology* **64**(92), 170–180. https://doi.org/10.1017/aog.2023.26

Received: 12 December 2022
Revised: 20 March 2023
Accepted: 21 March 2023
First published online: 3 May 2023

Keywords:
Antarctic glaciology; ice/ocean interactions; iceberg calving; icebergs

Corresponding author:
Olav Orheim, E-mail: olav@polarviten.no

cambridge.org/aog

Quantifying dissolution rates of Antarctic icebergs in open water

Olav Orheim[1], A. Barry Giles[2], T. H. (Jo) Jacka[3] and Geir Moholdt[1]

[1]Norsk Polarinstitutt, 9296 Tromsø, Norway; [2]Institute for Marine and Antarctic Studies (IMAS), University of Tasmania, Private Bag 80, Hobart, Tasmania 7001, Australia and [3]Antarctic Climate Program, Australian Antarctic Division, 203 Channel Highway, Kingston, Tasmania 7050, Australia

Abstract

At any one time 130 000 icebergs are afloat in the Southern Ocean; 97% of these are too small to be registered in current satellite-based databases, yet the melting of these small icebergs provides a major input to the Southern Ocean. We use a unique set of visual size observations of 53 000 icebergs in the South Atlantic Ocean, the SCAR International Iceberg Database, to derive average iceberg dissolution rates. Fracture into two parts is the dominant dissolution process for tabular icebergs, with an average half-life of 30 days for icebergs <4 km length and 60 days for larger icebergs. Complete shatter producing many icebergs <1 km length is rare. A side attrition rate of 0.23 m d^{-1} combined with drift speed of 6 km d^{-1}, or any proportional change in both numbers fits the observed changes in iceberg distribution. The largest injection into the Southern Ocean of fresh water and any iceberg-transported material takes place in a $\sim 2.3 \times 10^6$ km^2 zone extending east-northeast from the Antarctic Peninsula to the Greenwich meridian. The iceberg contribution to salinities and temperatures, with maximum contribution north of the Weddell Sea, differs in some regions, from those indicated by tracking large icebergs.

1. Introduction

Much of Antarctica's mass loss is by iceberg calving. Most of the mass calved is in the form of tabular icebergs >1 km length, and satellite technology provides several databases of these (Ballantyne and Long, 2002; Liu and others, 2015; Tournadre and others, 2015; Budge and Long, 2018). Although these databases have various limitations (cover only icebergs >18.5 km, do not cover regions of sea ice, cover only some years), in total they give a good understanding of the calving of large Antarctic icebergs.

To assess icebergs of all sizes, the systematic ship-based collection of iceberg data was initiated by the Norwegian Polar Institute and endorsed by the Scientific Committee on Antarctic Research (SCAR). By the 1982/1983 austral summer most research and supply ships within Antarctic waters were recording iceberg observations every 6 h in accordance with standardized instructions, and data up to 2010 are now compiled in the SCAR International Iceberg Database. The database contains 34 662 observations of 374 142 icebergs, of which 298 235 are classified into different size classes ranging from 10–50 m to >1 km. The database shows that in summer ~130 000 icebergs are afloat in the Southern Ocean, of which 97% have length <1 km. These smaller icebergs are not regularly recorded by satellites, even though different satellite sensors and products now have the capability of capturing icebergs much smaller than 1 km^2 (Zakharov and others, 2017; Qi and others, 2020; Shiggins and others, 2023).

The data were collected at 6-hourly intervals from a total of 233 ship cruises representing 20 nations using 68 vessels and involving >1000 observers over the collection period. Orheim and others (2022) describe the database and discuss uncertainties due to human error and other causes, which can be summarized as follows:

1) The length actually recorded for a distant iceberg depends on its dimensions, shape and the orientation to the observer.
2) The records were examined for repeat observations of extraordinary events (very large iceberg concentrations, very large icebergs) and duplications removed. Repeated observations from stationary ships were also deleted. The strength of the database is the large number of observations, and any incidental repeat observations of the same icebergs by different ships does not introduce statistical issues as long as average iceberg concentrations are discussed.
3) There is no evidence that the ship tracks were influenced by the presence of icebergs, while they are strongly affected by the presence of sea ice. This means that the data are mostly from open water situations, and most of the data are from the Antarctic summer and autumn. The tracks are also primarily from resupply ships travelling to the permanent research stations.
4) There is little evidence of human error in the records – instead the impression is that the personnel on the bridge of the ships took the task seriously.

2. Iceberg dissolution processes

Each time an iceberg fractures or loses mass by breakoff from the sides, the area exposed to melting is increased. The main iceberg melt input derives from the smaller icebergs that are 'children' of the initial larger icebergs. To ascertain input to the Southern Ocean of iceberg water and of any enclosed material, it is necessary to understand and to quantify the transition processes from large to small icebergs and to determine differences in drift between large and small icebergs. We use the SCAR database to delineate where most icebergs are found and to quantify dissolution rates.

Antarctic icebergs >250 m in length are assumed to be tabular, originating from ice shelves, and their dissolution is the main focus of the following discussion. Tabular icebergs disintegrate mainly by (a) underwater melting from the sides and base, (b) edge wasting from wave action at the waterline resulting in undercuts and small break-offs from the subaerial part and (c) fragmentation by fracture that splits the iceberg into two more or less equal parts or by shatter into numerous much smaller icebergs. Apart from underwater melting, the dissolution processes are insignificant when an iceberg is confined by sea ice, and the dissolution rates for most icebergs are very different in summer and winter. At air temperatures >0°C a drifting iceberg will also experience melting at the upper surface, but the meltwater will refreeze in the firn below as practically all Antarctic icebergs have internal temperatures <0°C leading to no run-off and no mass loss. Icebergs <250 m length calve mainly from the numerous Antarctic Peninsula glaciers but are also formed at the late stages of tabular iceberg disintegration. These icebergs will be prone to overturning, with melting as the main dissolution process.

Fragmentation is the most important yet least understood decay mechanism of tabular icebergs, being a stochastic process that makes individual events impossible to forecast (Bouhier and others, 2018). Prediction could be improved with knowledge of the flow history of the glacier from which the icebergs originated, but this is seldom available. There is a large difference in internal strength between broken-up small ice shelves like Stancomb-Wills Glacier Tongue, which produces small icebergs (Orheim, 1986), and the large ice shelves which episodically calve icebergs >500 km^2 on timescales of 10–100 years (MacAyeal and others, 2008). Tabular icebergs may fracture from swell-induced bending (Kristensen and others, 1982; Wadhams and others, 1983) in single or multiple divisions, perhaps along pre-existing faults, each time splitting into two or a few new, large icebergs. They may also fracture as a result of grounding or collision with other icebergs, as a result of bending due to hydrostatic forces (Reeh, 1968) or unbalanced buoyancy forces from underwater platforms (Orheim, 1987; Scambos and others, 2005; Wagner and others, 2014; Huth and others, 2022a), or from ocean-current shear (Huth and others, 2022b). Icebergs may also undergo rapid disintegration in a single-event shatter that produces many much smaller icebergs (Scambos and others, 2008). Importantly for this work, splitting and shattering give rise to very different size distributions.

Dissolution rates have previously been derived by comparing results of modeled iceberg melt and fracture rates with satellite databases (Gladstone and others, 2001; Wagner and others, 2017; Bouhier and others, 2018; England and others, 2020; Huth and others, 2022a). Iceberg melt rates depend primarily upon ocean temperature and current speed, and models have been developed pertaining to various environmental conditions. Published rates for underwater melting of icebergs in the open ocean range typically from ~0.05 m d^{-1} side melt (Jacka and Giles, 2007) for icebergs close to the continent, to >0.4 m d^{-1} basal melting of iceberg A68 (Braakmann-Folgmann and others, 2022) drifting in the South Atlantic from the Antarctic Peninsula to South Georgia. A melt rate of 0.4 m d^{-1} implies a loss of 146 m a^{-1} from the base. This seems high in view of observations of 200–250 m-thick icebergs persisting in the Antarctic Circumpolar Current (ACC) for much more than one year; an average melt rate of 0.2 m d^{-1} for icebergs drifting in open water seems more reasonable.

Parameterizing fracture events is much more difficult. Three large icebergs have been monitored closely by satellite (Scambos and others, 2008; Bouhier and others, 2018) leading to models for iceberg fragmentation. Given the stochastic nature of fragmentation however, any conclusions from such a small sample remain tentative. None of the models address the smaller icebergs that are most important for assessing total iceberg melt. This problem concerns both dissolution rates and distribution.

In addition to the approaches described above, dissolution rates might also be determined by following many icebergs over a drift period of many months using instruments or by detailed satellite monitoring, but such methods require large resources and have not yet been attempted. Here, we investigate instead whether iceberg dissolution rates can be quantified from the changes that a large population undergoes during drift. Fragmentation increases iceberg numbers and significantly changes the size distribution, while edge wasting and melting only slowly change the size distribution yet do not change numbers. Analyzing the changes in numbers and sizes of a confined drifting iceberg population can then give direct information on the relative importance of attrition and fragmentation processes. This expands on the approach used by Jacka and Giles (2007) to derive dissolution rates by analyzing data for icebergs drifting around and off-shore of East Antarctica.

3. Deriving dissolution rates using the drift of a confined iceberg population

3.1 Distribution and drift of icebergs in the Southern Ocean

Monitoring the drift of tabular icebergs has been carried out initially utilizing transponders (Vinje, 1980; Tchernia and Jeannin, 1984) and later from satellite observations; e.g. England and others (2020) have presented daily positions of icebergs >5 km size for the period 1992–2019. Antarctic icebergs generally follow the counter-clockwise coastal current until they leave the continent in exit zones and enter the clockwise ACC, but there can be significant deviations caused by winds and currents. Because the Coriolis effect is greatest for the largest icebergs, they tend to veer more to the left than smaller icebergs. With a deeper draft than smaller icebergs, changes in current with depth may also affect large iceberg drift differently than that of smaller icebergs.

Figure 1, modified from Figure 6 of Orheim and others (2022), shows the iceberg concentration around Antarctica and the major iceberg exit zones, within which icebergs leave the coastal currents to drift into the Southern Ocean. The exit zones are regions extending >500 km from the coast characterized by pronounced differences in iceberg densities, from high concentration inside the zone compared with low levels in adjoining grid boxes. Exit zone 3 is the physically largest and has also the largest set of iceberg observations, containing icebergs that derive from the Antarctic Peninsula and icebergs that have drifted north from the western Weddell Sea after originally calving further east. This zone is investigated further in the following analysis and discussion.

https://doi.org/10.1017/aog.2023.26 Published online by Cambridge University Press

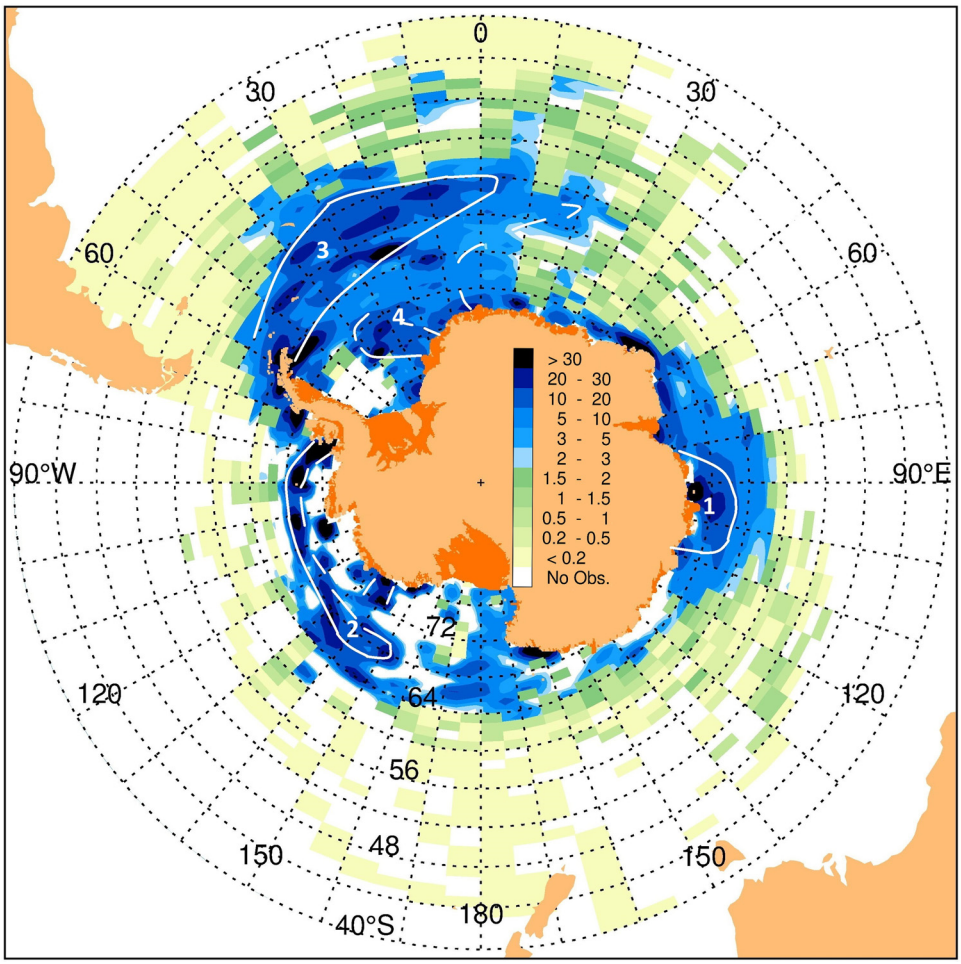

Figure 1. Iceberg concentration around Antarctica in 1° latitude × 5° longitude boxes. Major iceberg exit zones 1–4 are outlined in white. Concentration is defined as the sum of icebergs observed in a box divided by the number of observations. Green areas are locations of one or a few observations, and have higher uncertainty, particularly north of 50°S. White areas denote that no icebergs were observed or that there were zero observations. In Figures 1 and 2 the 1° × 5° box distributions have been contoured using the IDL software routine MIN_CURVE_SURF, which interpolates and smooths sets of regularly gridded but incomplete data.

3.2 The iceberg data in exit zone 3

Exit zone 3 extends more than 3000 km east-northeast of the northern tip of the Antarctic Peninsula, ranging south to north from 64° to 53°S and west to east from 55°W to 0° (Fig. 2).

To investigate the changes along the drift path, we compile all data collected in this zone independent of when they were collected and we make three assumptions: (1) that all observations are equally representative, (2) that the different times of observation do not preclude compiling them and (3) that the icebergs move in a confined corridor into which no new icebergs enter. The first assumption can be justified by the large number of observations (2893). The second assumption can be separated into two parts. Compiling data independent of year of collection means that year-to-year variations are discounted; the practical reality of this is borne out by the changes in frequencies being very much larger than any year-to-year variation in iceberg numbers presented in the SCAR database. Compiling data independent of when in the year they are collected means ignoring the effect of real seasonal changes in iceberg density (Orheim, 1980). This is justified because the data cover all months from spring to autumn, and because the changes in concentration are much larger than seasonal effects. With regards to the third assumption, Figures 1 and 2 and discussion below show that this assumption is only partially fulfilled, as there is likely influx of icebergs into the zone. At the same time, the data show that dissolution-caused changes in numbers and concentration along the drift paths dominate over any random effects caused by iceberg influx. It is therefore concluded that the data can be considered as an instantaneous view of the icebergs in the exit zone and that this gives a good basis for making quantitative calculations of dissolution processes.

Altogether 53 606 size-classified icebergs were recorded in the exit zone. In addition to these, another 1265 observations were made of 11 108 icebergs not classified by size, so that in the whole exit zone there were 4158 observations of 64 714 icebergs yielding 15.6 icebergs per observation. Figure 3 and the Appendix (Table 2) show how the observations vary with the segments. Particularly, the two largest sizes show a marked decline in numbers along the drift trajectories.

The relatively low iceberg densities evident in Figure 3 for segments 1–3 compared with the latter segments reflect that a large proportion of icebergs in the western Weddell Sea do not drift close to shore, a feature also shown by the satellite-tracks of large icebergs (Stuart and Long, 2011). In addition, there is influx (Fig. 2) from the north into segment 4, of icebergs drifting from the western side of the Antarctic Peninsula around the South Shetland and South Orkney Islands. Segment 4 is therefore taken as the starting point for the calculations below regarding the changes with time of the iceberg population in exit zone 3.

From segment 4 onwards, a general reduction in concentration for all size classes is evident, but with spikes caused by influx of icebergs from the central Weddell Sea. Satellite tracking shows that while nearly all large icebergs hug the coastline from 20°E to ~10°W, their drift directions differ thereafter. Many icebergs

https://doi.org/10.1017/aog.2023.26 Published online by Cambridge University Press

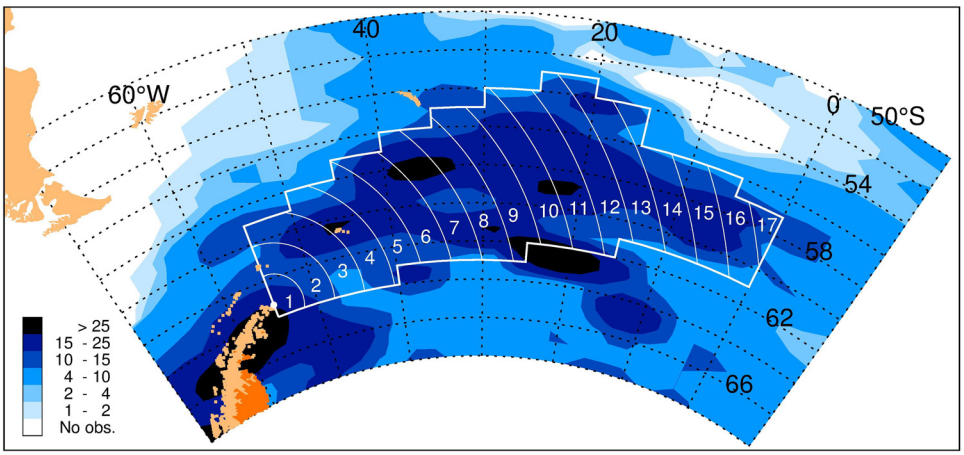

Figure 2. Iceberg concentrations in exit zone 3, which is divided into 17 segments of 178 km width, shown in white. The eastern point of Joinville Island at 63°20′S, 55°W (small dot), is taken as the end point of the Antarctic Peninsula. Note South Shetland Islands (~61–63°S), South Orkney Islands (~60°30′S) and South Georgia (~54°30′S). The zone consists of 73 1° × 5° grid boxes with a total area of 2.312×10^6 km^2. Its northern boundary is quite sharp, while the southern boundary is more diffuse because of the influx of icebergs from the central Weddell Sea, discussed further below.

drift into the southern Weddell Sea and these end up leaving the continent close to the northeastern tip of the Peninsula. Other icebergs leave the coastal current into exit zone 4 (Fig. 1). Schodlok and others (2006) showed that the drift of 52 GPS-tracked icebergs in the Weddell Sea varied greatly in direction from year to year, and that some drifted north into the central part of exit zone 3. These icebergs give rise to the spikes in density seen at segments 7, 10 and 14.

There are few data on drift speeds for small icebergs, but data on larger icebergs tracked utilizing transponders or satellites give consistent values and can be used as good indicators. The most comprehensive set of data in this region is provided by Schodlok and others (2006), who give drift rates ranging from 2.9 to 12.2 km d^{-1} for different iceberg populations, but with large individual variations. Collares and others (2018) give an average drift speed of 5.5 km d^{-1} for satellite-tracked icebergs in the northwestern Weddell Sea. A drift speed of 5.93 km d^{-1} is used in the following calculations. Taking 5.93 km d^{-1} is done for numerical convenience as this results in the icebergs taking 30 d to cross from one segment to the next. As will be shown later, it is the combination of drift speed and melt rates that is most important, and the initial choice of drift speed is not critical for the following discussions.

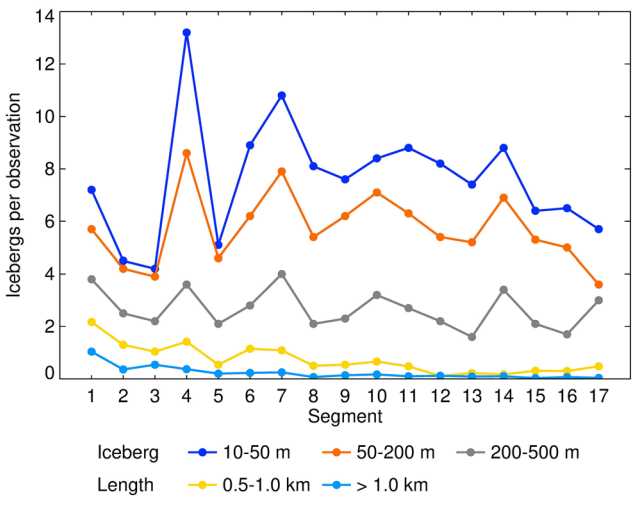

Figure 3. Concentration of icebergs vs segment distance from the Antarctic Peninsula.

The travel distance from segment 1 to 17 is ~3000 km. An iceberg must therefore drift for more than one year to reach segment 17, mostly in open water. In the summer, the minimum sea-ice extent is south of 64°S in this part of the Southern Ocean, while in winter, the sea-ice maximum reaches to between 55° and 60°S. Essentially all the ship-based iceberg observations were made in open water, and the results presented apply to open water situations.

3.3. Producing 'normalized' data to reduce random observational errors

The slight increase in ocean temperature from segment 4 to 17 is without abrupt change. There are also no other reasons to expect abrupt change in dissolution rates in the drift zone. We assume changes in iceberg distribution and dissolution during the drift from segment 4 to 17 are continuous, and that the variations shown in Figure 3 derive from random effects. To remove these variations, 'normalized' changes in iceberg concentration with distance are computed from the Appendix (Table 2) using linear regression fits. Figure 4a and the Appendix (Table 3) show the derived number of icebergs in each segment for an initial starting population set at 10 000 icebergs.

The observations presented in Figure 3, normalized in Figure 4, show that counter-intuitively, the proportion of smallest icebergs increases with time, even though most icebergs in size classes 1 and 2 in segment 4 are melted (to <10 m length) before reaching segments 7 and 16, respectively. This demonstrates that repeated fracture of larger icebergs occurs throughout the exit zone. As shown in more detail in the Appendix (Table 3), the percentage reduction is largest for the two largest iceberg sizes. Only 7% of size class 5 icebergs in segment 4 are found in segment 17. For class 4, the corresponding percentage is 11%. Thus, for the two largest classes, the main loss in size is caused by fragmentation, as attrition from the sides would only slowly shift some of these icebergs down one size class. Fragmentation on the other hand increases iceberg numbers, so that in the three smaller classes, numbers remain high at 65–75% of those in segment 4. Table 3 suggests that the half-life of icebergs decreases with drift from segment 4 to 17, but this is misleading. The >1 km icebergs in the different segments are not the same size, as the composition of the family of icebergs >1 km changes along the drift because fragmentation of the largest icebergs give rise to many new icebergs, all still belonging to the size class >1 km. This is illustrated below.

https://doi.org/10.1017/aog.2023.26 Published online by Cambridge University Press

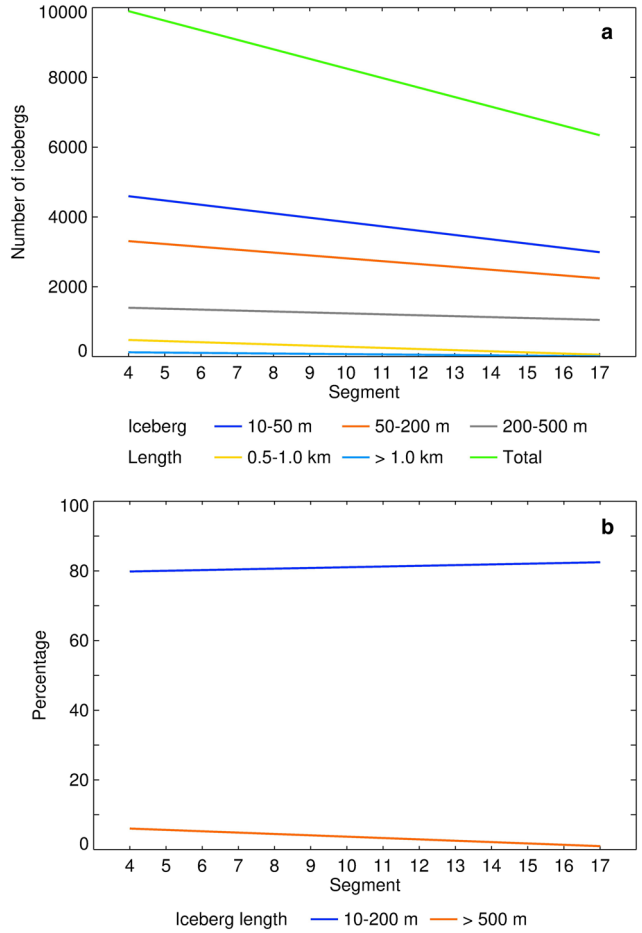

Figure 4. (a) Number of icebergs in each segment for a normalized population, initially of 10 000 icebergs. (b) Changes in percentages with travel distance for the normalized population of different sizes, from smallest (10–200 m) to largest (>500 m) icebergs.

Figure 5 shows that with increasing drift distance, there are changes in size distribution and a rapid fall-off in numbers of icebergs >1 km. The above sums of icebergs for the four groups of three segments are based on data presented in the Appendix (Table 4). No icebergs >6 km length are found beyond segment 9, and only icebergs <4 km persist into segment 12.

The observed icebergs in the five size classes are reasonably well represented by a linear fit on log–log scales of decreasing numbers with increasing size. Assuming the icebergs to be a

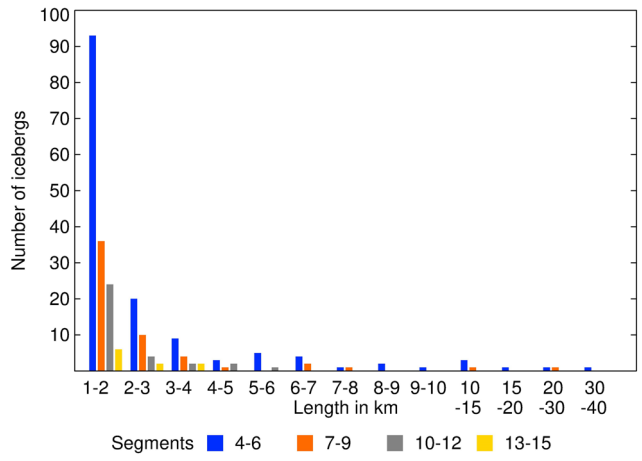

Figure 5. Number of observed icebergs of different lengths, in four groups (of different color), each of three segments.

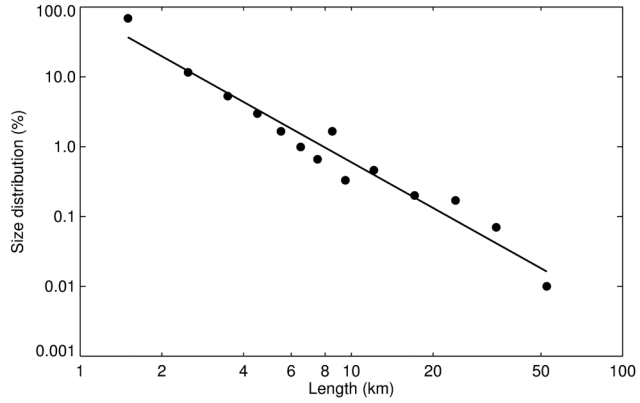

Figure 6. Size distribution of observed 302 icebergs >1 km in length as given in Appendix (Table 5), with axes drawn on logarithmic scales.

continuum of sizes, this scale could theoretically be extended to derive the length distribution of icebergs >1 km, but with obvious uncertainties. Fortunately, there are relevant observational data. The recording instructions for the observations asked that size be noted for icebergs >1 km, and this was done by many observers. Of the 818 icebergs >1 km within exit zone 3 (Appendix, Table 2), the length (and sometimes width and freeboard) was recorded for altogether 436 icebergs (Appendix, Table 4), including 302 in segments 1–4 which are taken as representative for the initial iceberg population. Their size distribution approximately follows a linear trend, when plotted on log–log scales (Fig 6). From these observations, we then calculate a normalized size distribution for the initial 123 icebergs >1 km, and use this to derive the initial size distribution for the large icebergs as shown in the Appendix (Table 5).

The linear relationship in Figure 6 follows a power law with a slope of −2.2. This relates to iceberg length, for iceberg area the slope would be −1.1, which is lower than the satellite-derived slope of −1.52 from Tournadre and others (2016). Further information on this size relationship is given in Supplementary Materials.

The complete SCAR dataset includes more than 3000 length observations of individual icebergs >1 km length. It would be of interest to compare these observations with the statistics of satellite observations, and to investigate how the size distribution of icebergs >1 km vary around the continent and between the different exit zones. Such studies are outside the scope of the present article.

3.4. Half-life for fracturing

The above has clarified that there is a marked reduction in tabular iceberg numbers with travel time in open water, so that practically all the largest icebergs in zone 3 have disappeared within one year of drift. Of the 49 icebergs >5 km length that were recorded, only one observation was beyond segment 7. In other words, after about half a year of travel in open water most large icebergs had disappeared, and all icebergs larger than 5 km had fractured at least once. Clearly fragmentation, rather than melting, is the overriding dissolution process, and the largest icebergs experience many fractures, to give rise to many 'children' of varying sizes.

Table 1 illustrates this process. Here the number of icebergs from segment 4 to 17 is added in groups of two to reduce random

Table 1. The observed icebergs >1 km grouped in pairs of segments (derived from the Appendix (Table 4)).

	Number of icebergs >1 km in each segment pair						
Segments	4–5	6–7	8–9	10–11	12–13	14–15	16–17
Total	130	41	29	27	10	6	4

https://doi.org/10.1017/aog.2023.26 Published online by Cambridge University Press

variations. No iceberg >1 km was observed in segment 17. The sum of icebergs >1 km is approximately halved in moving across two segments, implying the half-life of large icebergs is on average ~60 d. This half-life is used as the starting point in the following discussions.

It is not possible to clarify from the above whether fragmentation takes place in successive fracture events with a time spacing of days, weeks or months, or in a single event shattering into many pieces. Satellite records of break-up of spectacular giant icebergs indicate that both processes occur, however it is not clear how relevant this is for fragmentation of the mostly much smaller icebergs discussed here. Smaller icebergs formed as a by-product of splitting of large icebergs are also frequently noted in satellite studies, e.g. Li and others (2018). However, the persistence of the two smallest sizes of icebergs into the easternmost segments indicates a repeated introduction of new small icebergs formed by fracture of larger icebergs; in other words, the largest icebergs have fractured in more than one event, spaced weeks or months apart.

3.5. Quantifying the dissolution processes

The changes in iceberg population with travel time in open water in exit zone 3 can now be used to investigate dissolution processes and rates, taking as a starting point the normalized iceberg population given in the Appendix (Tables 3, 5). The changes from segment 4 to 16 place constraints on fragmentation and melt rates, thus limiting boundary conditions for simulations. For example, the persistence of high numbers of small icebergs means that there must be larger icebergs undergoing fracture throughout the exit zone.

We assume icebergs are evenly distributed in length within a size class and simulate the changes in iceberg population evolving during drift by numerical iteration of changes in the iceberg population travelling from segment 4 to 16. Details of the iteration are given in Supplementary Table S1. The iteration starts with the following boundary conditions based on earlier discussions and on general knowledge of iceberg behavior in open water.

1. *Drift rate*: 5.93 km d^{-1}.
2. *Attrition rate*: Taken as 0.2 m d^{-1} for iceberg sides and base in segment 4, increasing gradually to 0.26 m d^{-1} in segment 16 because of warmer waters. Wave action makes the side attrition larger than the basal melt, as described earlier. The effect of this is discussed below but is not important for the immediate discussion.
3. *Fracture sizes*: An iceberg that fractures is taken to split into two iceberg 'children' of ~equal length.
4. *Fracture rate and half-life for icebergs >0.5 km*: Icebergs 0.5–4 km long are given a half-life of 30 d, meaning 75% are split after 60 d. Icebergs >4 km length are given an average half-life of 60 d, i.e. half the icebergs >4 km are split after travel across two segments.
5. *Fracture rate for icebergs <0.5 km*: Dissolution by attrition increases in importance as the length decreases, and only 25% of icebergs 0.2–0.5 km length are assumed to fracture after 60 d.
6. *Small icebergs as by-products of fracture*: Each fracture is taken to produce as a by-product three icebergs <50 m length.
7. *Shattering rate*: In each segment from 5 to 13, it is assumed that one iceberg of size 4–8 km shatters completely into icebergs of 0.5–1 km length. This rate is chosen to make the simulation fit observations. The resulting nine icebergs represent 2% of the icebergs >1 km length.

Discussion of the boundary condition chosen for the simulations:

(1) and (2) As shown above, the observed iceberg drift rates in the region vary considerably, and different, most probably higher, rates could be chosen. However, the iceberg numbers clarify that attrition and drift correlate, e.g. a 50% increase in drift rate would also require a 50% increase in attrition rate to match the iceberg distribution throughout the exit zone. Average attrition rates can be deduced from known iceberg drift rates, but without that knowledge any appropriate combination of the two rates will achieve an acceptable fit. The numbers chosen here are within the range of observed rates.

(3) Icebergs >0.5 km can be assumed to be tabular. Introducing choices of unequal lengths after splitting do not significantly change these calculations.

(4) and (5) The choices of half-lives for the simulations are constrained within a fairly narrow range to arrive at iceberg numbers that are consistent with observed distribution throughout the exit zone.

(6) Personal observations and literature descriptions of tabular iceberg fracture show that small icebergs are a by-product of break-up, but there are no data to indicate quantities. We chose a factor of three as reasonable, and because it makes our simulations fit observations.

(7) With regards to shattering rate, good fits could be achieved also by different combinations of shatter numbers, size and drift time, but within clear limits. Shattering the largest icebergs is not realistic as this would give too large a deviation from the observed sum for class 1–4 icebergs. Letting all shattered icebergs have size 0.5–1 km is likely not realistic but allows simple calculation of the number of generated 'children', which is proportional to the ratio of the area of original to new icebergs, i.e. length^2, assuming the same average length/width ratio. But changing the shattering parameters will not necessarily provide new insight. The important take-away is that complete shatter must only affect a small proportion of the tabular icebergs, and not include the largest of these.

Simulations based on these boundary conditions closely reproduce the normalized observations, as shown by Figure 7 and the Appendix (Table 6). The decreases in numbers are closely mirrored, and most numbers for all size classes and segments agree within ~±10%. This indicates that these boundary conditions are close to reality. Given the number of assumptions underlying this numerical exercise, we do not aim to fine-tune to get closer fits, even though this could easily be achieved by assuming different size composition of the 'children' after fracture. We further note that one realistic explanation that would reduce the deviation for size class 2 (50–200 m) is that a proportion of these icebergs undergo fracture. In the simulation above fracture has only been assigned to tabular icebergs >200 m. In reality, many icebergs <200 m while not tabular, nevertheless have shapes, such as 'dry-dock', that lead to fracture. The fracture model applied here assumes that the splitting divides the iceberg length, but we note that after a number of such reductions in length the initial width would likely become the longest side. Compensating for this effect would only have minor impact on the simulated numbers. Some icebergs may drift at higher speeds, which would imply longer drift distance before disintegration. The rapid fall-off in iceberg numbers east of the Greenwich meridian in the SCAR database suggests that a large increase in drift speed combined with unchanged attrition rate is not realistic. Proportionally increasing speed and attrition rate would lead to unchanged results, but after shorter travel times. Large changes in attrition rate alone are not commensurate with the changes in iceberg population. Higher attrition rates from wave action at the sides compared with basal melt results in overturning events occurring sooner in the lifetime of small tabular icebergs; this is included in

https://doi.org/10.1017/aog.2023.26 Published online by Cambridge University Press

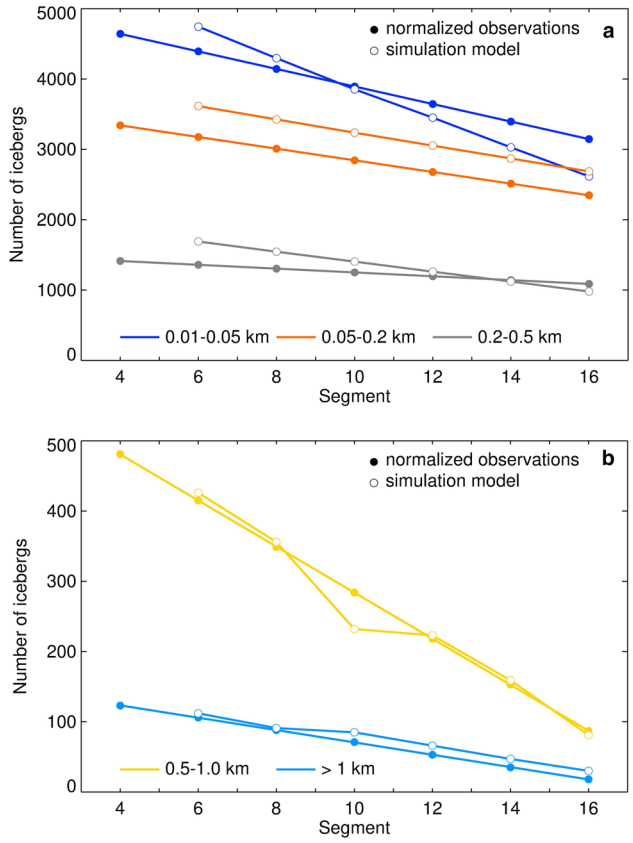

Figure 7. Normalized and simulated number of icebergs from segment 4 to 16 for the five size classes. The normalized observations start at segment 4, the simulated at segment 6. Exact numbers are given in the Appendix (Table 6). (a) Size classes 1–3, (b) size classes 4 and 5.

the simulations by assigning that only 25% of 200–500 m icebergs are fractured after 60 d.

The ship-based observations of the extensive presence of small icebergs after a year of drift in open water provide a boundary framework relevant for discussions of iceberg dissolution based on satellite databases referred to above. Analyses that ignore fracturing and relate dissolution processes mainly to melting (e.g. Rackow and others, 2017) will result in iceberg lives and trajectories not consistent with the observations presented here. These results also have potential for quantifying further iceberg fragmentation theory (e.g. Åström and others, 2021).

3.6 Iceberg contribution to the Southern Ocean

3.6.1 Regional differences in ocean impact concluded from satellite and ship-based observations

As already indicated, the SCAR iceberg database distributions differ from satellite-derived distributions in some regions. As an overarching remark, we note that studies that use satellite iceberg databases to estimate iceberg impacts on the Southern Ocean need to take into account the following two aspects: Firstly, the differences between visual and satellite observations are particularly large in the Pacific sector. Here the satellite records of icebergs >5 km for the 1992–2019 period (England and others, 2020) show more large icebergs emerging from the Ross Sea than from the Bellingshausen Sea/Amundsen Sea region, whereas the SCAR database indicates the opposite. The relatively few ship observations do not allow precise delineation of the southern boundary of exit zone 2 (Fig. 1) and the calving sources. However, they clearly indicate high calving rates in this sector in the observation period, possibly of relevance to present discussions of the stability of glaciers in this region. Perhaps the differences from satellite observations are a result of relatively more icebergs <5 km length calving from glaciers feeding exit zone 2. Secondly, as the largest icebergs veer furthest north in the ACC, the satellite data may indicate iceberg dissolution and fresh water input further north than actually occurs. The magnitude of this can be assessed by comparing the iceberg distribution in exit zone 3 (Fig. 2) with, e.g. Figure 4 of Silva and others (2006) or Figure 2 of Rackow and others (2017).

3.6.2 Effect on Southern Ocean temperatures and salinities

The long-term mean iceberg production rate can be approximated by the observed steady-state ice flux along Antarctica's calving fronts, which has been estimated to be in the range 1.265×10^{12} m^3 a^{-1} to 1.411×10^{12} m^3 a^{-1} water (Depoorter and others, 2013; Rignot and others, 2019; Greene and others, 2022). The year-to-year variability in iceberg production can be of a similar order of magnitude owing to the infrequent calving of giant icebergs, with the last major calving cycle occurring in the years between 2000 and 2002 when large parts of the fronts of the two largest ice shelves in Antarctica, Ross and Filchner-Ronne, calved off. Over the past quarter of a century, the net loss of ice shelf mass has averaged around 0.25×10^{12} m^3 a^{-1} which would add another 15–20% to the steady-state iceberg production rate. Where these icebergs disintegrate and melt in the Southern Ocean, they provide fresh water that reduces temperatures and salinities. Evenly distributed over the 36×10^6 km^2 area of the Southern Ocean, the annual iceberg production represents a rate of injection of 0.04 m^3 m^{-2}, an order of magnitude less than the contribution from precipitation minus evaporation (P–E) (Turner and others, 1999).

However, the dissolution of Antarctic icebergs is not evenly distributed within the Southern Ocean. Stuart and Long (2011) concluded that 90% of all large tabular icebergs end up in the Weddell Sea, and as shown here, thereafter mostly in exit zone 3. The data in the SCAR Iceberg Database (Orheim and others, 2022) suggest that 90% may be too high, and many icebergs also in the Weddell Sea region drift outside exit zone 3 as defined here. Nevertheless, taking a conservative estimate that 50% of the large icebergs ends up in exit zone 3, this results in a total of 0.7×10^{12} m^3 iceberg water. With an area of 2.3×10^6 km^2 implying an average local injection rate ~0.3 m^3 m^{-2} in exit zone 3. The maximum ice melting in the zone takes place from segment 4 to 14, i.e. from 50°W to 10°W. Here the iceberg contribution exceeds precipitation minus evaporation and needs to be taken into account in ocean models.

3.6.3. Biological impact

Icebergs also carry terrigenous nutrients which supply most of the iron input to the Southern Ocean (Death and others, 2014; Wu and Hou, 2017). It is no coincidence that the region of exit zone 3 is, according to statistics from the Convention on the Conservation of Antarctic Marine Living Resources (CCAMLR), also the region from which the largest catches of krill are obtained, and where most whales were caught in the days before whaling became prohibited. Further discussion of how the iceberg dissolution results presented relate to biological productivity is however, outside the scope of this article.

3.6.4. Iceberg hazards to shipping

The results presented here have direct implications on iceberg hazards to shipping in the South Atlantic. Real hazards stem from growlers (<5 m length) which are difficult to see at night or in poor visibility, and yet large enough to penetrate the hull of a ship travelling at full speed. Thus, in the austral summer, the dangers are largest in the northern part of the Southern

https://doi.org/10.1017/aog.2023.26 Published online by Cambridge University Press

Ocean, where the nights are long. Icebergs large enough to be seen by radar are, on the other hand, normally not a hazard. Combining ship routes (e.g. McCarthy and others, 2022) with the iceberg distribution analysis presented here provides control on any theoretical assessments of iceberg hazards (e.g. Bigg and others, 2018). Particularly relevant are the observations of small icebergs as by-products of fracturing, and the persistence of small icebergs throughout the exit zone.

4. Results and conclusions

In the above, we have shown that analysis of the iceberg distribution data in exit zone 3 clarifies fundamental issues related to the dissolution processes of icebergs in open water. While the exact numbers used are not critical, the dataset is large enough to make robust conclusions. The observations of the smallest icebergs define boundaries for the attrition melt rate, while the observations of the largest icebergs clarify the relative importance of splitting rather than shattering for these sizes.

We conclude that the following parameters apply for the dissolution of icebergs travelling in open water in exit zone 3, from near the Antarctic Peninsula to 0°W:

- a side attrition/melt rate of 0.2 m d^{-1} in segment 4, increasing to 0.26 m d^{-1} in segment 16 combined with a drift speed of 6 km d^{-1}. A higher attrition rate would need a corresponding increase in drift speed.
- repeated splitting into two parts is the dominant fragmentation process of tabular icebergs.
- the half-life for splitting is ~30 d for icebergs 0.5–4 km long, and averages 60 d for icebergs >4 km.
- each iceberg split produces an additional average of three small iceberg 'children' <50 m in length.
- only ~2% of icebergs >1 km length are completely shattered into many icebergs <1 km in length, and those icebergs that shatter are 4–8 km in length.

The above average half-lives hide large individual variations in iceberg strength and fracture rates. A gradually increasing half-life with increasing size is probably more realistic than the one-step increase at 4 km used in the calculations, and conforms with the rare observations of large icebergs circumnavigating the continent. Nevertheless, we suggest that these rates give a realistic quantification of iceberg dissolution processes for a family of many icebergs in this part of the Southern Ocean, which could be of value to oceanographic researchers and others who want to parameterize iceberg decay. The simulations show that repeated splitting into two parts is the dominant fracture process for larger icebergs, and that the choice of half-lives is most important to match observations. We suggest that these rates can be taken as representative averages for any large iceberg population in the open Southern Ocean, outside the sea-ice zone. These results follow the conclusion of England and other (2020), that to simulate the effect of icebergs on the Southern Ocean, it is critical to include both large tabular icebergs and a representation of their breakup beyond the standard decay models.

The smallest icebergs are the sources of most ice melting, and their distributions show that the largest impacts are in the northern part of the Atlantic sector of the Southern Ocean.

Supplementary material. The supplementary material for this article can be found at https://doi.org/10.1017/aog.2023.26

Data availability. The SCAR International Iceberg Database is free-access available from the SCAR data depository and from https://doi.org/10.21334/npolar.2021.e4b9a604.

Acknowledgements. We extend our gratitude to the SCAR nations for carrying out the ship observation program. Comments from two anonymous reviewers, the Scientific Editor and the Chief Editor significantly improved this paper.

References

Åström J and 5 others (2021) Fragmentation theory reveals processes controlling iceberg size distributions. *Journal of Glaciology* **67**(264), 603–612. doi: 10.1017/jog.2021.14

Ballantyne J and Long DG (2002) A multidecadal study of the number of Antarctic icebergs using scatterometer data. Proceedings of International Geoscience and Remote Symposium (IGARSS) Toronto, Canada, 24–28 June 2002. doi: 10.1109/IGARSS.2002.1026859

Bigg GR and 9 others (2018) A model for assessing iceberg hazard. *Natural Hazards* **92**(2), 1113–1136. doi: 10.1007/s11069-018-3243-x

Bouhier N, Tournadre J, Rémy F and Gourves-Cousjin R (2018) Melting and fragmentation laws from the evolution of two large Southern Ocean icebergs estimated from satellite data. *The Cryosphere* **12**, 2267–2285. doi: 10.5194/tc–12–2267–2018

Braakmann-Folgmann A, Shepherd A, Gerrish L, Izzard J and Ridout A (2022) Observing the disintegration of the A68A iceberg from space. *Remote Sensing of Environment* **270**, 112855. doi: 10.1016/j.rse.2021.112855

Budge JS and Long DG (2018) A comprehensive database for Antarctic iceberg tracking using scatterometer data. *IEEE Journal of Selected Topics in Applied Earth Observations and Remote Sensing* **11**, 434–442. doi: 10.1109/JSTARS.2017.2784186

Collares LL, Mata MM, Kerr R, Arigony-Neto J and Barbat MM (2018) Iceberg drift and ocean circulation in the northwestern Weddell Sea, Antarctica. *Deep Sea Research Part II: Topical Studies in Oceanography* **149**, 10–24. doi: 10.1016/j.dsr2.2018.02.014

Death R and 7 others (2014) Antarctic ice sheet fertilises the Southern Ocean. *Biogeosciences* **11**, 2635–2643. doi: 10.5194/bg-11-2635-2014

Depoorter MA and 6 others (2013) Calving fluxes and basal melt rates of Antarctic ice shelves. *Nature* **502**, 89–92. doi: 10.1038/nature12567

England M, Wagner TJW and Eisenman I (2020) Modeling the breakup of tabular icebergs. *Science Advances* **6**(51), eabd1273. doi: 10.1126/sciadv.abd1273

Gladstone RM, Bigg GR and Nichols KW (2001) Iceberg trajectory modeling and meltwater injection in the Southern Ocean. *Journal of Geophysical Research* **106**(c9), 19903–19915. doi: 10.1029/2000JC000347

Greene CA, Gardner AS, Schlegel N and Fraser AD (2022) Antarctic calving loss rivals ice-shelf thinning. *Nature* **609**, 948–953. doi: 10.1038/s41586-022-05037-w

Huth A, Adcroft A and Sergienko O (2022a) Parameterizing tabular-iceberg decay in an ocean model. *Journal of Advances in Modeling Earth Systems* **14**, e2021MS002869. doi: 10.1029/2021MS002869

Huth A, Adcroft A, Sergienko O and Khan N (2022b) Ocean currents break up a tabular iceberg. *Science Advances* **8**, 1–5. doi: 10.1126/sciadv.abq6974

Jacka TH and Giles AB (2007) Antarctic iceberg distribution and dissolution from ship-based observations. *Journal of Glaciology* **53**(182), 341–356. doi: 10.3189/002214307783258521

Kristensen M, Squire V and Moore S (1982) Tabular icebergs in ocean waves. *Nature* **297**, 669–671. doi: 10.1038/297669a0

Li T and 5 others (2018) Monitoring the tabular icebergs C28A and C28B calved from the Mertz Ice Tongue using radar remote sensing data. *Remote Sensing of Environment* **216**, 615–625. doi: 10.1016/j.rse.2018.07.028

Liu Y and 7 others (2015) Ocean-driven thinning enhances iceberg calving and retreat of Antarctic ice shelves. *Proceedings of the National Academy of Sciences of the USA* **112**(11), 3263–3268. doi: 10.1073/pnas.1415137112

MacAyeal DR and 5 others (2008) Tabular iceberg collisions within the coastal regime. *Journal of Glaciology* **54**, 371–386. doi: 10.3189/002214308784886180

McCarthy AH, Peck LS and Aldridge DC (2022) Ship traffic connects Antarctica's fragile coasts to worldwide ecosystems. *Proceedings of the National Academy of Sciences of the USA* **119**, e2110303118. doi: 10.1073/pnas.2110303118.

Orheim O (1980) Physical characteristics and life expectancy of tabular Antarctic icebergs. *Annals of Glaciology* **1**, 11–18. doi: 10.3189/S0260305500016888

Orheim O (1986) Flow and thickness of Riiser-Larsenisen, Antarctica. *Norsk Polarinstitutt Skrifter* **16**, 5–20. http://hdl.handle.net/0/1

Orheim O (1987) Evolution of under-water sides of ice shelves and icebergs. *Annals of Glaciology* **9**, 176–182. doi: 10.3189/S0260305500000574

Orheim O, Giles AB, Moholdt G, Jacka TH (Jo) and Bjørdal A (2022) Antarctic iceberg distribution revealed through three decades of systematic ship-based observations in the SCAR International Iceberg Database. *Journal of Glaciology*, 1–15. doi: 10.1017/jog.2022.84

Qi M and 5 others (2020) Efficient location and extraction of the iceberg calved areas of the Antarctic ice shelves. *Remote Sensing* **12**(16), 2658. doi: 10.3390/rs12162658

Rackow T and 5 others (2017) A simulation of small to giant Antarctic iceberg evolution: differential impact on climatology estimates. *Journal of Geophysical Research – Oceans*, **122**, 3170–3190. doi: 10.1002/2016JC012513

Reeh N (1968) On the calving of ice from floating glaciers and ice shelves. *Journal of Glaciology* **7**(50), 215–232. doi: 10.3189/S0022143000031014

Rignot E and 5 others (2019) Four decades of Antarctic ice sheet mass balance from 1979–2017. *The Proceedings of the National Academy of Sciences* **116**(4), 1095–1103. doi: 10.1073/pnas.1812883116

Scambos T and 7 others (2008) Calving and ice-shelf break-up processes investigated by proxy: Antarctic tabular iceberg evolution during northward drift. *Journal of Glaciology* **54**, 579–591. doi: 10.3189/002214308786570836

Scambos T, Sergienko O, Sargent A, MacAyeal D and Fastook J (2005) ICESat profiles of tabular iceberg margins and iceberg breakup at low latitudes. *Geophysical Research Letters* **32**, L23S09. doi: 10.1029/2005GLO23802

Schodlok MP, Hellmer HH, Rohardt G and Fahrbach E (2006) Weddell Sea iceberg drift: five years of observations. *Journal of Geophysical Research* **111**, C06018. doi: 10.1029/2004JC002661

Shiggins CJ, Lea JM and Brough S (2023) Automated ArcticDEM iceberg detection tool: insights into area and volume distributions, and their potential application to satellite imagery and modelling of glacier–iceberg–ocean systems. *The Cryosphere* **17**, 15–32. doi: 10.5194/tc-17-15-2023

Silva TAM, Bigg GR and Nicholls KW (2006) Contribution of giant icebergs to the Southern Ocean freshwater flux. *Journal of Geophysical Research* **111**, 1–8. doi: 10.1029/2004JC002843

Stuart KM and Long DG (2011) Tracking large tabular icebergs using the SeaWinds Ku-band microwave scatterometer. *Deep Sea Research* **11**(58), 1285–1300. doi: 10.1076/dsr2.2010.11.004

Tchernia P and Jeannin PF (1984) Circulation in Antarctic waters as revealed by iceberg tracks, 1972–1983. *Polar Record* **22**, 263–269. doi: 10.1017/S0032247400005386

Tournadre J, Bouhier N, Girard-Ardhuin F and Rémy F (2015) Large icebergs characteristics from altimeter waveforms analysis. *Journal of Geophysical Research - Oceans* **120**, 2121–2128. doi: 10.1002/2014JC010502

Tournadre J, Bouhier N, Girard-Ardhuin F and Rémy F (2016) Antarctic icebergs distributions 1992–2014. *Journal of Geophysical Research – Oceans* **121**, 327–349. doi: 10.1002/2015JC011178

Turner J, Connolley WM, Leonard S, Marshall GJ and Vaughan DG (1999) Spatial and temporal variability of net snow accumulation over the Antarctic from ECMWF re-analysis project data. *International Journal of Climatology* **19**, 697–724. doi: 10.1002/(SICI)1097-0088(19990615)19:7<697::AID-JOC392>3.0.CO;2-3

Vinje TE (1980) Some satellite-tracked iceberg drifts in the Antarctic. *Annals of Glaciology* **1**, 83–87. doi: 10.3189/S026030550001702X

Wadhams P, Kristensen M and Orheim O (1983) The response of Antarctic icebergs to ocean waves. *Journal of Geophysical Research* **88**(C10), 6053–6065. doi: 10.1029/jc088ic10p06053

Wagner TJW, Dell RW and Eisenman I (2017) An analytical model of iceberg drift. *Journal of Physical Oceanography* **47**(7), 1605–1616. doi: 10.1175/JPO-D-16-0262.1

Wagner TJW, Wadhams P and 7 others (2014) The 'footloose' mechanism: iceberg decay from hydrostatic stresses. *Geophysical Research Letters* **41**(15), 5522–5529. doi: 10.1002/2014GL060832

Wu SJ and Hou S (2017) Impact of icebergs on net primary productivity in the Southern Ocean. *The Cryosphere* **11**, 707–722. doi: 10.5194/tc-11-707-2017

Zakharov I, Puestow T, Fleming A, Deepakumara J and Power D (2017) Detection and discrimination of icebergs and ships using satellite altimetry. In 2017 IEEE International Geoscience and Remote Sensing Symposium (IGARSS), 882–885. doi: 10.1109/IGARSS.2017.8127093

https://doi.org/10.1017/aog.2023.26 Published online by Cambridge University Press

Appendix

Table 2. Observed iceberg distribution in the 17 segments of exit zone 3 (Fig. 2)

	Segment																	
	1	2	3	4	5	6	7	8	9	10	11	12	13	14	15	16	17	1–17
Dist.	178	365	534	712	890	1068	1246	1424	1602	1780	1958	2136	2314	2492	2670	2848	3026	Total
Iceberg observations																		
Class 1	852	1173	1115	7790	992	1364	1649	1325	1696	2211	1095	743	514	520	392	540	154	24 125
Class 2	668	1084	1028	5044	896	944	1195	873	1366	1882	784	495	357	408	322	411	96	17 853
Class 3	453	638	573	2130	407	430	613	340	516	835	334	196	112	200	129	143	81	8130
Class 4	256	338	276	837	105	176	165	82	120	174	59	10	15	10	19	25	13	2680
Class 5	123	93	142	218	38	35	38	11	30	46	12	11	6	6	2	6	1	818
Tot. class	2352	3326	3134	16 019	2438	2949	3660	2631	3728	5148	2284	1455	1004	1144	864	1125	345	53 606
Tot. obs.	118	260	265	589	193	153	152	163	222	264	124	91	69	59	61	83	27	2893
Concentration % (icebergs per Class in segment / Total No. of observations)																		
Class 1	7.2	4.5	4.2	13.2	5.1	8.9	10.8	8.1	7.6	8.4	8.8	8.2	7.4	8.8	6.4	6.5	5.7	
Class 2	5.7	4.2	3.9	8.6	4.6	6.2	7.9	5.4	6.2	7.1	6.3	5.4	5.2	6.9	5.3	5.0	3.6	
Class 3	3.8	2.5	2.2	3.6	2.1	2.8	4.0	2.1	2.3	3.2	2.7	2.2	1.6	3.4	2.1	1.7	3.0	
Class 4	2.17	1.3	1.04	1.42	0.54	1.15	1.09	0.5	0.54	0.66	0.48	0.11	0.22	0.17	0.31	0.3	0.48	
Class 5	1.04	0.36	0.54	0.37	0.20	0.23	0.25	0.07	0.14	0.17	0.10	0.12	0.09	0.10	0.03	0.07	0.04	

Distances are in km from Joinville Island. The concentrations are the number of classified icebergs per observation within the segment.

Table 3. Normalized distribution of icebergs in exit zone 3, based on the changes in distribution derived from the iceberg observations presented in Table 2

	Segment													
	4	5	6	7	8	9	10	11	12	13	14	15	16	17
Physical parameters														
Distance km	0	178	356	534	712	890	1068	1246	1424	1602	1780	1958	2136	2314
Drift days	0	30	60	90	120	150	180	210	240	270	300	330	360	390
Model – concentration: icebergs/observation														
Class 1	9.9	9.6	9.3	9.1	8.8	8.6	8.3	8.0	7.8	7.5	7.2	7.0	6.7	6.4
Class 2	7.1	6.9	6.8	6.6	6.4	6.2	6.1	5.9	5.7	5.5	5.3	5.2	5.0	4.8
Class 3	3.0	2.9	2.9	2.8	2.8	2.7	2.7	2.6	2.5	2.5	2.4	2.4	2.3	2.3
Class 4	1.02	0.95	0.88	0.81	0.74	0.67	0.6	0.53	0.46	0.39	0.33	0.26	0.19	0.12
Class 5	0.26	0.24	0.23	0.21	0.19	0.17	0.15	0.13	0.11	0.09	0.08	0.06	0.04	0.02
Total	21.3	20.7	20.1	19.5	18.9	18.3	17.8	17.2	16.6	16.0	15.4	14.8	14.2	13.6
Model – % of icebergs														
Class 1	46.4	46.5	46.5	46.5	46.6	46.6	46.7	46.7	46.8	46.8	46.9	47.0	47.1	47.1
Class 2	33.4	33.5	33.6	33.7	33.8	34.0	34.1	34.2	34.4	34.5	34.7	34.9	35.1	35.3
Class 3	14.1	14.3	14.4	14.5	14.7	14.8	15.0	15.2	15.3	15.6	15.8	16.0	16.3	16.5
Class 4	4.8	4.6	4.4	4.2	3.9	3.7	3.4	3.1	2.8	2.5	2.1	1.7	1.3	0.8
Class 5	1.2	1.2	1.1	1.1	1.0	0.9	0.8	0.8	0.7	0.6	0.5	0.4	0.3	0.1
Model – no. of icebergs normalized to 10 000 total in segment 4														
Class 1	4642	4517	4393	4268	4143	4018	3894	3769	3644	3520	3395	3270	3146	3021
Class 2	3341	3258	3175	3093	3010	2927	2844	2761	2678	2596	2513	2430	2347	2264
Class 3	1413	1386	1359	1331	1304	1277	1250	1223	1196	1168	1141	1114	1087	1060
Class 4	481	448	415	382	349	317	284	251	218	186	153	120	87	54
Class 5	123	115	106	97	88	79	71	62	53	44	35	27	18	9
Total	10 000	9724	9448	9171	8894	8618	8343	8066	7789	7514	7237	6961	6685	6408

The upper part of Table 3 shows the derived results for the segments, and the lower part gives the number of icebergs that should then be in each segment for an initial starting population set at 10 000 icebergs.

Table 4. Size distribution of observed icebergs of recorded length >1 km within the different segments of the exit zone

Length	Segment																	
km	1	2	3	4	5	6	7	8	9	10	11	12	13	14	15	16	17	Total
1–2	23	42	61	82	4	7	15	8	13	12	6	6	2	4	0	4	0	289
2–3	8	7	5	15	4	1	7	0	3	3	1	0	1	0	1	0	0	56
3–4	8	0	4	4	3	2	0	0	4	2	0	0	1	1	0	0	0	29
4–5	1	3	3	2	1	0	0	0	1	1	1	0	0	0	0	0	0	13
5–6	0	1	2	2	2	1	0	0	0	1	0	0	0	0	0	0	0	9
6–7	1	0	0	2	2	0	2	0	0	0	0	0	0	0	0	0	0	7
7–8	1	0	1	0	0	1	1	0	0	0	0	0	0	0	0	0	0	4
8–9	0	2	1	2	0	0	0	0	0	0	0	0	0	0	0	0	0	5
9–10	0	1	0	0	0	1	0	0	0	0	0	0	0	0	0	0	0	2
10–15	3	2	1	1	1	1	1	0	0	0	0	0	0	0	0	0	0	10
15–20	0	2	0	1	0	0	0	0	0	0	0	0	0	0	0	0	0	3
20–30	1	3	0	1	0	0	1	0	0	0	0	0	0	0	0	0	0	6
30–40	0	1	0	1	0	0	0	0	0	0	0	0	0	0	0	0	0	2
>40	0	0	1	0	0	0	0	0	0	0	0	0	0	0	0	0	0	1
Total	46	64	79	113	17	14	27	8	21	19	8	6	4	5	1	4	0	436

The 302 observed icebergs in segments 1–4 are used to construct a 'normalized' initial size distribution (see Table 5). Segments 1–4 are used instead of only segment 4 to reduce random observational effects. The >40 km iceberg was 65 km long.

https://doi.org/10.1017/aog.2023.26 Published online by Cambridge University Press

Table 5. Observed sizes of 302 icebergs, and normalized size distribution of 123 icebergs >1 km

Initial data (from Table 4) Normalized class 5 bergs in seg. 1–4						
Length	Segment		Midpoint			
km	1–4	%	km	%	Number	
1–2	208	68.9	1.5	54.1	66.5	67
2–3	35	11.6	2.5	17.4	21.4	21
3–4	16	5.3	3.5	8.4	10.3	10
4–5	9	3.0	4.5	4.85	6.0	6
5–6	5	1.7	5.5	3.15	3.9	4
6–7	3	1.0	6.5	2.20	2.8	3
7–8	2	0.7	7.5	1.65	2.0	2
8–9	5	1.7	8.5	1.26	1.6	2
9–10	1	0.3	9.5	1.00	1.2	1
10–15	7	2.3	10.5	0.81	1.0	1
15–20	3	1.0	11.5	0.65	0.8	1
20–30	5	1.7	12.5	0.56	0.7	0
30–40	2	0.7	13.5	0.48	0.59	1
>40	1	0.3	14.5	0.41	0.50	0
Total	302	100.0	15.5	0.35	0.43	1
			16.5	0.31	0.38	0
			17.5	0.28	0.34	0
			18.5	0.25	0.31	1
			19.5	0.22	0.28	0
			20.5	0.20	0.25	0
			22.0			1
			44.0			1
					Total	123

The first three columns of Table 5 give observed numbers and percentages of sum of icebergs in segments 1–4. The normalized initial population of 123 icebergs >1 km in segment 4 (column 5) is calculated from these percentages, assuming a regular logarithmic decrease in numbers with increasing size (123 icebergs >1 km is the initial number in class 5 for a total starting population of 10 000, Table 3). The penultimate column gives the iceberg distribution to one decimal point computed from these percentages. As only whole numbers can apply, either 0 or 1 is assigned for icebergs >10.5 km in the final column to, as far as possible, reflect the computed distribution.

Table 6. Normalized and simulated number of icebergs in segments 4–16

	Segment												
Length	4	N6	S6	N8	S8	N10	S10	N12	S12	N14	S14	N16	S16
10–50	4642	4393		4143		3894		3644		3395		3146	
			4744		4296		3853		3451		3028		2616
50–200	3341	3175		3010		2844		2678		2513		2347	
			3615		3426		3237		3053		2870		2686
200–500	1413	1359		1304		1250		1196		1141		1087	
			1690		1545		1404		1261		1121		979
500–1000	481	415		349		284		218		153		87	
			426		356		232		223		159		81
>1000 m	123	106		88		71		53		35		18	
			112		91		85		66		47		30

The simulated (S) numbers of icebergs of the five size classes for segments 6–16 and the normalized (N) numbers for an initial iceberg population of 10 000 (Table 3). The simulated numbers are calculated from the boundary conditions described in section 3.5. The detailed calculations are given in Supplementary Table S1.

https://doi.org/10.1017/aog.2023.26 Published online by Cambridge University Press